Groundwater seepage is a key driver of theater-headed valley formation in limestone

Aaron Micallef[1,2]*, Nader Saadatkhah[1], Jurgen Spiteri[2], Enzo Rizzo[3,4], Luigi Capozzoli[4], Gregory De Martino[4], Letizia Pace[4], Christine Burrill[5], Michael Gatt[2], Mark Schmidt[1] and Shubhangi Gupta[1]

[1]Helmholtz Centre for Ocean Research, GEOMAR, 24148 Kiel, Germany
[2]Department of Geosciences, University of Malta, Msida MSD 2080, Malta
[3]Department of Physics and Earth Science, University of Ferrara, 44122 Ferrara, Italy
[4]CNR-IMAA, Laboratorio Hydrogeosite, Tito-Marsico Nuovo 85050, Italy
[5]Department of Earth and Environmental Science, New Mexico Institute of Mining and Technology, Socorro, New Mexico 87801, USA

ABSTRACT

Groundwater seepage leads to the formation of theater-headed valleys (THVs) in unconsolidated sediments. In bedrock, the role of groundwater in THV development remains disputed. Here, we integrate field and remote-sensing observations from Gnejna Valley (Maltese Islands) with numerical modeling to demonstrate that groundwater seepage can be the main driver of THV formation in jointed limestone overlying clays. The inferred erosion mechanisms entail (1) widening of joints and fractures by fluid pressure and dissolution and (2) creeping of an underlying clay layer, which lead to slope failure at the valley head and its upslope retreat. The latter is slower than the removal of the talus by creep and sliding on the valley bed. The location and width of THVs are controlled by the location of the master fault and the extent of the damage zone, respectively. The variability of seepage across the fault zone determines the shape of the valley head, with an exponential decrease in seepage away from the fault giving rise to a theater-shaped head that best matches that of Gnejna Valley. Our model may explain the formation of THVs by groundwater in jointed, strong-over-weak chemical sedimentary lithologies, particularly in arid terrestrial settings.

INTRODUCTION

Whereas field observations and experimental/numerical simulations have shown that groundwater seepage can lead to the formation of theater-headed valleys (THVs) in sand and gravel, the mechanism for their development in consolidated bedrock remains controversial (Lamb et al., 2006; Lapotre and Lamb, 2018; Lobkovsky et al., 2007; Micallef et al., 2021; Ryan and Whipple, 2020). The classic model for the formation of THVs in bedrock entails weathering at the seepage face, which weakens the rock and renders grains cohesionless; these grains are subsequently removed by seeping water, leading to undermining, collapse, and retreat (Dunne, 1980; Laity and Malin, 1985). Arguments against the role of groundwater in the formation of THVs in clastic sedimentary or non-sedimentary rocks include: (1) the large size of some THVs, (2) time required for extensive weathering, and (3) inability of spring discharge

to remove the talus (Lamb et al., 2006; Lapotre and Lamb, 2018). Groundwater weathering and erosion processes in different types of bedrock have not been quantified in terms of mechanisms and rates. A diagnostic link between groundwater seepage and geometry of bedrock THVs remains unclear and poorly quantified (Petroff et al., 2011). Reasons for such gaps in knowledge include: (1) field observations and experimental simulations are difficult—the time scales involved are long and the processes are complex; (2) experimental and numerical analyses have been based on simplistic assumptions about flow processes and hydraulic characteristics, and they rarely simulate effects of geologic heterogeneities; and (3) an unambiguous example of a THV formed by groundwater seepage in bedrock is lacking because of overlapping features generated by rainfall runoff. In addition, bedrock THVs are not uniquely associated with groundwater. Groundwater seepage may be complemented by surface-water erosion, or the latter may be enough to explain bedrock THV formation,

e.g., in substrate with stratigraphic contrasts and vertical joints, waterfall erosion through plunge-pool erosion or plucking/toppling, and megaflooding (Lamb et al., 2008, 2007, 2006, 2014; Nash, 1996; Ryan and Whipple, 2020; Scheingross and Lamb, 2017). Elucidating the association between groundwater seepage and bedrock THVs is crucial to reconstructing/predicting landscape evolution, with direct relevance to hazard assessment, and to inferring past climates and fluvial conditions.

In this study, we combine field and remote-sensing observations from the Maltese Islands with numerical modeling to demonstrate that groundwater seepage can be the main driver of THV formation in limestone. We infer the mechanisms responsible and the factors controlling THV location, shape, and size.

REGIONAL SETTING

The Maltese Islands comprise four main Oligo-Miocene sedimentary formations (Pedley et al., 1976; Fig. 1A). Lower Coralline Limestone (Chattian) and Globigerina Limestone (Aquitanian to Langhian) consist of shallow-water marine calcareous algae and deep-water planktonic foraminifera, respectively. Blue Clay (Langhian to Tortonian) is composed of banded kaolinitic marls and clays. Upper Coralline Limestone (late Tortonian to early Messinian) is subdivided into four members: Gebel Imbark, Tal-Pitkal, Mtarfa, and Ghajn Melel. Tal-Pitkal Member is a coarse-grained wackestone and packstone containing coralline algal, mollusc, and echinoid bioclasts. Mtarfa Member consists of massive to thickly bedded carbonate mudstone and wackestone rich in coralline algae. The entire sedimentary sequence is disrupted by two normal fault systems, the most
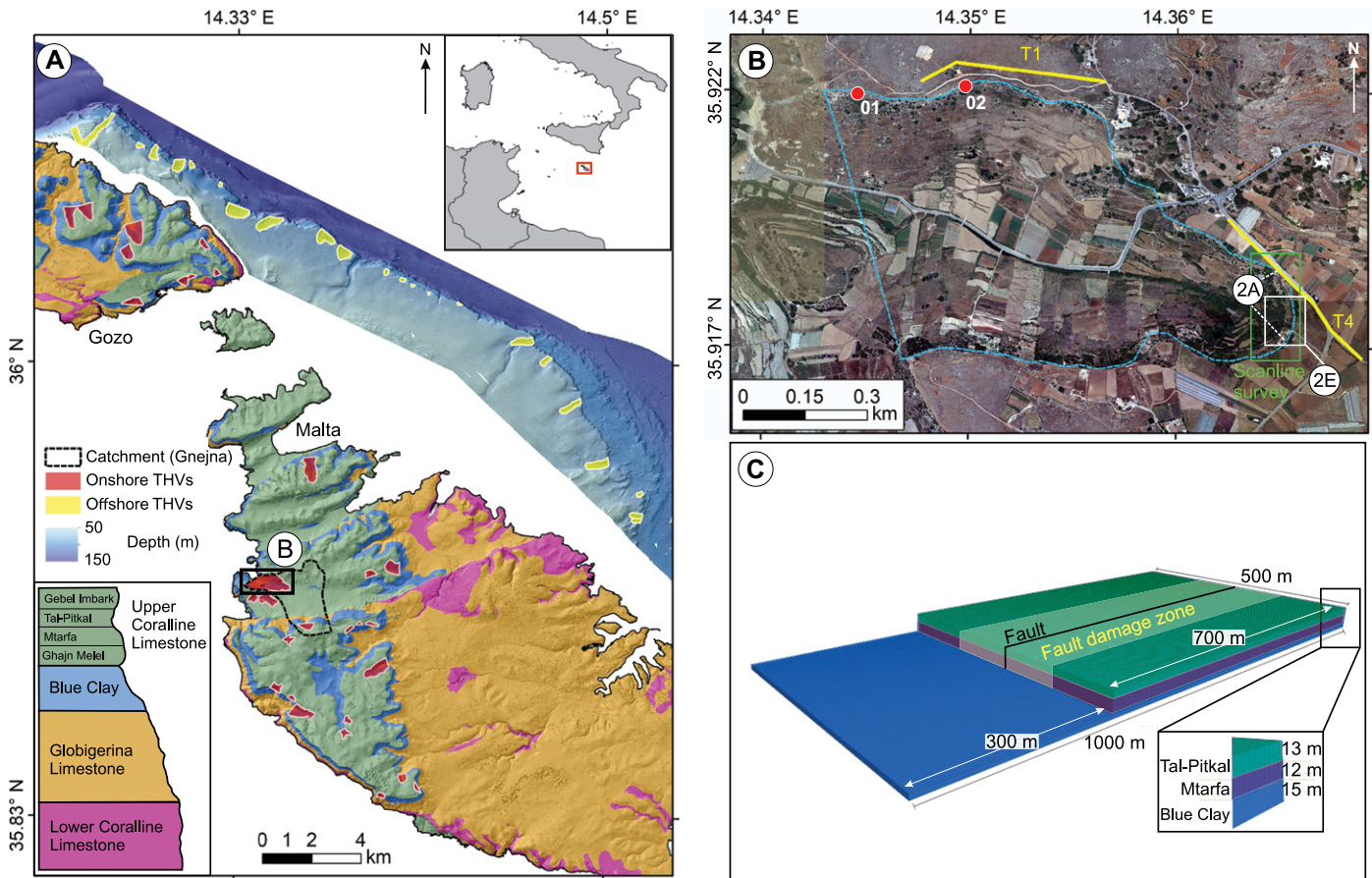
*E-mail: amicallef@geomar.de

Figure 1. (A) Location, geological, and bathymetric map of the Maltese Islands. Locations of theater-headed valleys (THVs) and the catchment of Gnejna Valley are denoted. Shaded relief and bathymetry data are from Micallef et al. (2013, 2019). **(B)** Orthophotograph of Gnejna Valley (marked in dashed blue line). Yellow lines T1 and T4 are the electrical resistivity tomography (ERT) and ground penetrating radar (GPR) profiles. Locations of samples for cosmogenic nuclide dating and scanline survey are denoted by red dots and the green rectangle, respectively. Locations of Figures 2A and 2E are shown in white. **(C)** Three-dimensional distinct element model domain.

widespread of which consists of ENE-WSW–trending faults dipping at 55°–75° (Illies, 1981).

The Maltese Islands have a semiarid climate, with a mean annual precipitation of 550 mm (Galdies, 2011). Lower Coralline Limestone hosts the mean-sea-level groundwater, whereas Upper Coralline Limestone hosts perched groundwater bodies above Blue Clay (Bakalowicz and Mangion, 2003).

All THVs considered in this study occur in Upper Coralline Limestone (Fig. 1A; Haroon et al., 2021). Onshore THVs are associated with natural springs fed by perched groundwater, and most of them are oriented parallel to known faults. One of these THVs—Gnejna Valley in northwestern Malta (Fig. 1A)—was selected as a case study because of its size and accessibility. The mean temperature, conductivity, and pH of perched groundwater at Gnejna Valley for 2009–2017 CE are 19.7 °C, 1420 μS/cm, and 7.5, respectively. Offshore THVs are thought to have formed subaerially because they were exposed during the Last Glacial Maximum and are draped by 5–10 m of hemipelagic sediment accumulated since then (Micallef et al., 2013).

MATERIALS AND METHODS

Topographic lidar and multibeam echosounder data are available for the entire Maltese Islands and for the seafloor to as much as 150 m depth, respectively (Micallef et al., 2013, 2019; Fig. 1A). These data were used to map onshore and offshore THVs. Gnejna Valley was surveyed with an uncrewed aerial vehicle to generate orthophotos and elevation models with a horizontal resolution of 10 cm/pixel (Fig. 1B; Fig. S1 in the Supplemental Material[1]). Electrical resistivity tomography (ERT) and ground penetrating radar (GPR) data were acquired along two 470-m-long profiles located to the north and east of Gnejna Valley, respectively, to map the underlying stratigraphy, structure, and groundwater (Fig. 1B). A 250-m-long scanline survey was carried out at the base of the head of Gnejna

[1]Supplemental Material. Detailed description of the field data collection methods, sample analyses, and numerical modeling. Please visit https://doi.org/10.1130/GEOL.S.19232964 to access the supplemental material, and contact editing@geosociety.org with any questions.

Valley (Fig. 1B) to estimate orientation, spacing, and roughness of discontinuities (ISRM, 1978, 1985). Rock-wall strength was measured with an N-type Schmidt hammer. Surface samples of Upper Coralline Limestone and Blue Clay were taken from the head and northern rim of the valley for scanning electron microscopy, measurement of geotechnical/hydraulic properties, and cosmogenic nuclide dating (Fig. 1B).

Hydrological modeling entailed estimation of (1) groundwater discharge at Gnejna Valley using GIS hydrology tools and (2) surface discharge required to transport boulders in the valley using continuity, Manning, and Shields equations. A landscape evolution model, based on Chen et al. (2014), was developed to assess the effect of erosion by surface flow on valley development. Three-dimensional (3-D) distinct element modeling was carried out on a 1000 m × 500 m × 40 m domain using 3DEC modeling code (Fig. 1C) and accounted for elastic hydromechanical widening, dissolution of joints/fractures in limestone, sliding of limestone blocks, and creep in clay (Barton, 1972; Garcia-Rios et al., 2015; Hoek and Bray, 1981; Roscoe and Burland, 1968).

Detailed information on the data and methods used is available in the Supplemental Material.

RESULTS AND DISCUSSION
Field and Remote-Sensing Observations

We identified 53 THVs: 30 across Malta and Gozo, and 23 offshore the northeastern coast (Fig. 1A). THVs have U-shaped cross-sections and linear longitudinal profiles; valleys widen downstream at a mean rate of 0.67 m width per 1 m length ($\sigma = 0.65$). With a length of 1.5 km, width of 0.85 km, and relief of 75 m, Gnejna Valley is the largest THV (Fig. 1B). The valley head and flanks are formed in Tal-Pitkal and Mtarfa Members dipping at $<1°$ to the west-northwest, whereas the bed predominantly consists of Blue Clay (Fig. 2A). The head of Gnejna Valley is a near-vertical, 25-m-high wall characterized by vertical joints and fractures (Fig. 2A; Fig. S3; geomechanical properties in Table S2 in the Supplemental Material). At the base of the head, water seeps out of joints and fractures and a talus of Upper Coralline Limestone boulders, mainly >1.5 m in diameter, has formed (Fig. 2A). Mtarfa Member outcropping at the valley head and flanks is characterized by a recess with evidence of spalling (Figs. 2B and 2D). Dissolution occurs only in the inner faces of joints and fractures (Fig. 2C). Surface exposure ages for samples 01 and 02 are 11.1 and 33.4 ka, respectively (Table S6).

Electrical resistivity tomography (ERT) profiles show a shallow, 10–30 m high-resistivity layer (>600 Ωm), a ~5 m intermediate-resistivity layer (100–300 Ωm), and a deeper, low-resistivity layer (<50 Ωm) (Fig. 2G; Fig. S2). Via correlation with outcrops, we interpret these layers as unsaturated Upper Coralline Limestone, saturated Upper Coralline Limestone (i.e., containing perched groundwater), and Blue Clay, respectively. The southeastern section of profile T4 shows an offset that corresponds with a west-east–trending fault throwing 15 m toward the south (Fig. 2G) and with the location of the main spring. GPR profiles show quasi-vertical master joints and fractures in Upper Coralline Limestone and a decrease in electromagnetic signal amplitude associated with perched groundwater (Fig. 2G; Fig. S2).

Processes Forming Gnejna Valley

Based on the above data, we dismiss three hypotheses for THV formation at Gnejna Valley:

(1) Detachment of valley head by surface flow: Apart from a 20-m-wide and 90-m-long V-shaped channel above the valley head (Fig. 2E), there is a lack of well-developed channels draining toward Gnejna Valley (Fig. 1A; Fig. S1). Fluvial abrasion marks and plunge pool undercuttings are absent (Figs. 2E and 2F). Landscape evolution modeling suggests that erosion by surface flow would form a valley with a pointed head, which is different from Gnejna Valley (Fig. S5).

(2) Erosion by megafloods: Features cited in support of megaflooding, such as scours and flood deposits, are absent. In addition, the orientation of THV axes is variable (Fig. 1A). There are no records of megafloods across the Maltese Islands, and factors responsible for such events elsewhere (e.g., rapid melting of ice sheets,
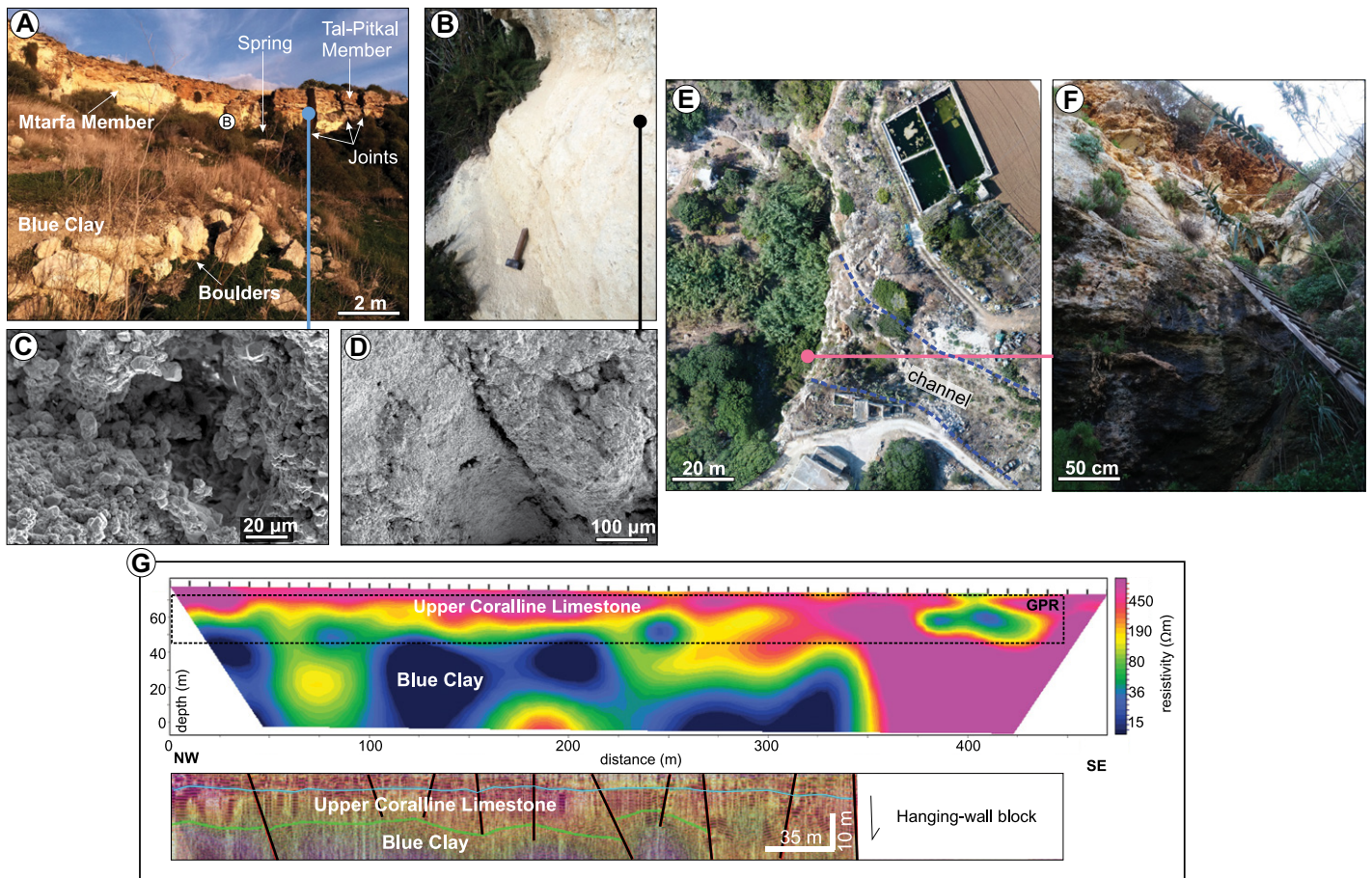

Figure 2. (A) Photograph of the Gnejna Valley head showing vertical cliff, outcropping geological layers, joints, boulders, and spring. Location from which the photograph was taken is shown in Figure 1B. (B) Recess in the Mtarfa Member at Gnejna Valley head. (C,D) Scanning electron microscope images of dissolution in the inner face of the joint (C) and spalling in the recess (D). Locations are shown in A and B. (E) Ortho-photograph (location in Fig. 1B) showing small channel at the top of the Gnejna Valley head. (F) Photograph of the base of the Gnejna Valley head (location in E) (looking upward at the vertical wall at the head from the base). (G) Electrical resistivity tomography and ground penetrating radar (GPR) profiles for line T4 (location in Fig. 1B). Interpreted joints/fractures are denoted by black solid lines. Boundary between the Upper Coralline Limestone and Blue Clay is marked by the green line, whereas the top of perched groundwater is marked by the light blue line.
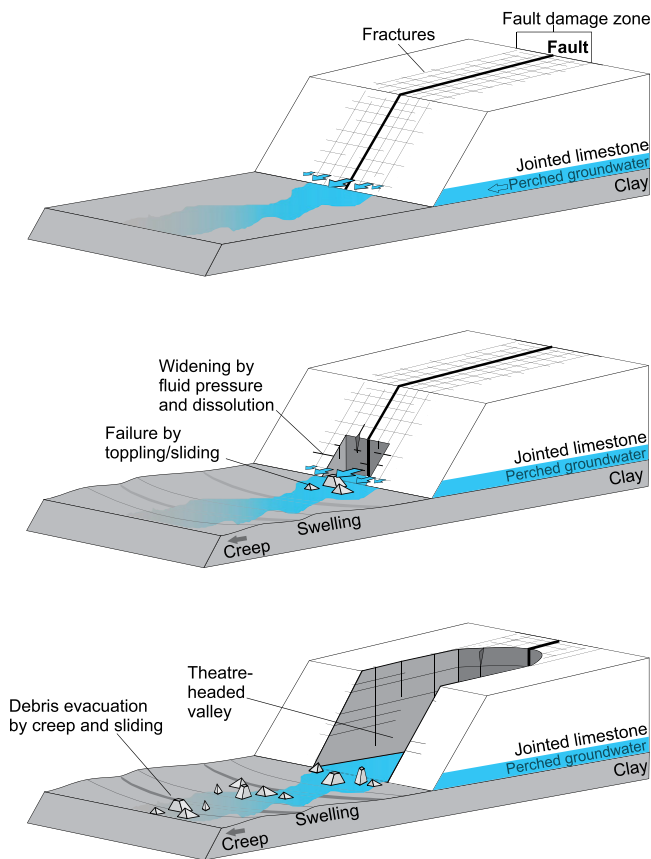
Figure 3. Schematic model for the formation of theater-headed valleys in jointed limestone overlying clays.

ice-dammed lake failure) have been absent here in the last 5 m.y.

(3) Groundwater weathering at a seepage face, leading to undermining and loss of support: Groundwater seeps through the joints/fractures rather than the low-permeability matrix. Recesses are pervasive across Mtarfa Member outcrops everywhere, including other sites and not just at the head of Gnejna Valley, and their formation is likely associated with

mechanical weathering by wetting and drying (Figs. 2B and 2D).

We propose an alternative mechanism by which Gnejna Valley was formed (Fig. 3). Development and upslope retreat of the THV head in Upper Coralline Limestone takes place via slope failure—toppling or sliding—driven by groundwater seepage via joints and fractures. The latter gives rise to: (1) widening of valley head–orthogonal joints and fractures by fluid pressure and dissolution, which reduces Upper Coralline Limestone's mass strength; and/or (2) creep of Blue Clay, which leads to loss of support at the base of the THV head. Failed material is transported downslope and away from the head by creep of Blue Clay (driven by seepage and precipitation) and sliding. We test the effectiveness of this mechanism in forming THVs using 3-D distinct element modeling.

Numerical Simulations

We consider the above two groundwater-related processes individually and together. Given that faulting appears to control the location of seepage (Fig. 2), we also assess the role played by fault-zone permeability (Caine et al., 1996). Four modes of groundwater seepage are examined: (1) point seepage (at the fault), and (2) no change, (3) linear decrease, and (4) exponential decrease in seepage away from the fault and across the fault damage zone (Fig. 1C). The latter mode is based on the exponential increase in fracture spacing with fault-normal distance, which is commonly reported in the literature and observed at Gnejna Valley (Liao et al., 2019; Sagy et al., 2001; Fig. S3). Simulations taking into account increased seepage across the fault damage zone (modes 2–4) result in valleys similar to THVs across the Maltese Islands, widening downstream at rates of 0.6–2 m width per 1 m length (Fig. 4). However, simulations for mode 4 give rise to a head morphology that is most similar to that of Gnejna Valley and most other THVs. The width of the fault damage zone controls the maximum width of the THV. Both widening of joints and fractures in Upper Coralline Limestone and creep of Blue Clay are effective processes driving THV formation. The estimated THV head retreat rate is 0.72–1.32 cm/yr. Surface exposure ages suggest retreat rates of 1.8–7.1 cm/yr (calculated by dividing axial distance of sampling sites from THV head by age). We would expect actual retreat rates to be closer to 1.8 cm/yr because the young age recorded at sampling site 01 was likely due to a recent slope failure.

The talus accumulating on the THV bed needs to be removed to ensure that head retreat is not hindered (e.g., Dunne, 1990; Lapotre and Lamb, 2018). The 3-D distinct element model yields creep and sliding rates of 1–62 cm/yr for a 1.5 m Upper Coralline Limestone boulder on Blue Clay sloping 1°–20° (Fig. S6). Considering that the slope gradient of Blue Clay in Gnejna Valley is 2°–6.3° and that it likely reached 20°
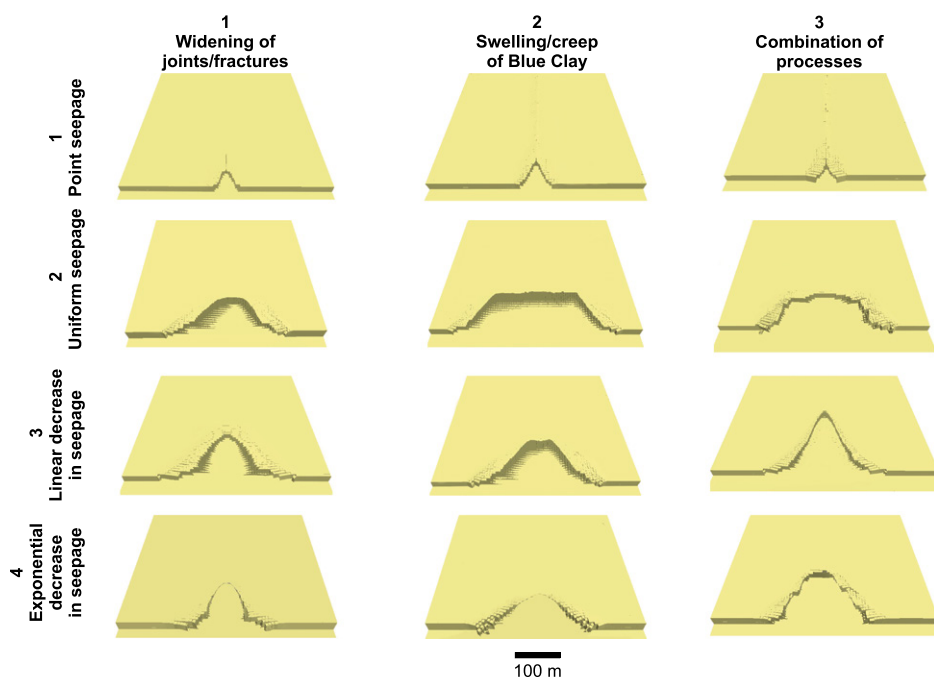

Figure 4. Theater-headed valley morphology derived from a three-dimensional distinct element model for four modes of groundwater seepage across fault damage zone (vertical axis) and for three processes (horizontal axis). Detached blocks were removed to aid visualization.

at the coast prior to THV formation, the transport rates of 1.5 m boulders on the Gnejna Valley bed have generally been higher than head retreat rates. Spring discharge (estimated at 0.01 m³/s) is too low to remove these boulders. A flash flood generated by a rainfall event of at least 10.3 m/day would be required to transport such boulders (Supplemental Material section 3.1), which is unrealistic. The largest boulders that may have been transported by documented flash floods (rainfall of 100 mm/day) are ~10 cm in diameter.

Estimates of rates for THV head retreat and boulder transport are based on current annual precipitation. Past climate variability in the Maltese Islands is poorly constrained, and its exclusion limits the accuracy of our estimates. On the other hand, factors promoting head retreat (e.g., increased annual rainfall) are expected to promote removal of talus as well.

CONCLUSIONS

We demonstrate how groundwater seepage can be the main driver of THV formation in jointed limestone overlying clays. By integrating field and remote-sensing observations from the Maltese Islands with numerical modeling, we show that groundwater seepage due to a permeability contrast can widen joints and fractures in limestone and promote creep of the underlying clay. Both of these processes lead to development and retreat of a THV head by slope failure. Talus is removed by creep and sliding on the valley bed at a rate faster than that of head retreat. By concentrating groundwater seepage across a cliff face, faults control the location of THVs. The maximum width of the THV is determined by the width of the fault damage zone, whereas the shape of the head is controlled by how seepage changes away from the fault core. An exponential decrease of seepage gives rise to a theater-shaped head that is similar to that of Gnejna Valley. Our model may explain the formation of THVs by groundwater in jointed, strong-over-weak chemical sedimentary lithologies, particularly in arid terrestrial settings.

REFERENCES CITED
Bakalowicz, M., and Mangion, J., 2003, The limestone aquifers of Malta: Their recharge conditions from isotope and chemical surveys, *in* Servat, E., et al., eds., Hydrology of the Mediterranean and Semiarid Regions: International Association of Hydrological Sciences Publication 278, p. 49–54.

Barton, N.R., 1972, A model study of rock-joint deformation: International Journal of Rock Mechanics and Mining Sciences, v. 9, p. 579–582, https://doi.org/10.1016/0148-9062(72)90010-1.

Caine, J.S., Evans, J.P., and Forster, C.B., 1996, Fault zone architecture and permeability structure: Geology, v. 24, p. 1025–1028, https://doi.org/10.1130/0091-7613(1996)024<1025:FZAPS>2.3.CO;2.

Chen, A., Darbon, J., and Morel, J.-M., 2014, Landscape evolution models: A review of their fundamental equations: Geomorphology, v. 219, p. 68–86, https://doi.org/10.1016/j.geomorph.2014.04.037.

Dunne, T., 1980, Formation and controls of channel networks: Progress in Physical Geography, v. 4, p. 211–239, https://doi.org/10.1177/030913338000400204.

Dunne, T., 1990, Hydrology, mechanics, and geomorphic implications of erosion by subsurface flow, *in* Higgins, C.G., and Coates, D.R., eds., Groundwater Geomorphology: The Role of Subsurface Water in Earth-Surface Processes and Landforms: Geological Society of America Special Paper 252, p. 1–28, https://doi.org/10.1130/SPE252-p1.

Galdies, C., 2011, The Climate of Malta: Statistics, Trends and Analysis 1951–2010: Valletta, Malta, National Statistics Office, 45 p.

Garcia-Rios, M., Luquot, L., Soler, J.M., and Cama, J., 2015, Influence of the flow rate on dissolution and precipitation features during percolation of CO_2-rich sulfate solutions through fractured limestone samples: Chemical Geology, v. 414, p. 95–108, https://doi.org/10.1016/j.chemgeo.2015.09.005.

Haroon, A., et al., 2021, Electrical resistivity anomalies offshore a carbonate coastline: Evidence for freshened groundwater?: Geophysical Research Letters, v. 48, e2020GL091909, https://doi.org/10.1029/2020GL091909.

Hoek, E., and Bray, J.W., 1981, Rock Slope Engineering: New York, Elsevier Science Publishing, 364 p.

Illies, J.H., 1981, Graben formation—The Maltese Islands—A case history: Tectonophysics, v. 73, p. 151–168, https://doi.org/10.1016/0040-1951(81)90182-7.

ISRM (International Society for Rock Mechanics Commission on Standardization of Laboratory and Field Tests), 1978, Suggested methods for the quantitative description of discontinuities in rock masses: International Journal of Rock Mechanics and Mining Sciences & Geomechanics Abstracts, v. 15, p. 319–368, https://doi.org/10.1016/0148-9062(78)91472-9.

ISRM (International Society for Rock Mechanics Commission on Standardization of Laboratory and Field Tests), 1985, Suggested method for determining point load strength: International Journal of Rock Mechanics and Mining Sciences & Geomechanics Abstracts, v. 22, p. 51–60, https://doi.org/10.1016/0148-9062(85)92327-7.

Laity, J.E., and Malin, M.C., 1985, Sapping processes and the development of theater-headed valley networks in the Colorado Plateau: Geological Society of America Bulletin, v. 96, p. 203–217, https://doi.org/10.1130/0016-7606(1985)96<203:SPATDO>2.0.CO;2.

Lamb, M.P., Howard, A.D., Johnson, J., Whipple, K.X., Dietrich, W.E., and Perron, J.T., 2006, Can springs cut canyons into rock?: Journal of Geophysical Research, v. 111, E07002, https://doi.org/10.1029/2005JE002663.

Lamb, M.P., Howard, A.D., Dietrich, W.E., and Perron, J.T., 2007, Formation of amphitheater-headed valleys by waterfall erosion after large-scale slumping on Hawai'i: Geological Society of America Bulletin, v. 119, p. 805–822, https://doi.org/10.1130/B25986.1.

Lamb, M.P., Dietrich, W.E., Aciego, S.M., DePaolo, D.J., and Manga, M., 2008, Formation of Box Canyon, Idaho, by megaflood: Implications for seepage erosion on Earth and Mars: Science, v. 320, p. 1067–1070, https://doi.org/10.1126/science.1156630.

Lamb, M.P., Mackey, B.H., and Farley, K.A., 2014, Amphitheater-headed canyons formed by megaflooding at Malad Gorge, Idaho: Proceedings of the National Academy of Sciences of the United States of America, v. 111, p. 57–62, https://doi.org/10.1073/pnas.1312251111.

Lapotre, M.G.A., and Lamb, M.P., 2018, Substrate control on valley formation by groundwater on Earth and Mars: Geology, v. 46, p. 531–534, https://doi.org/10.1130/G40007.1.

Liao, Z.H., Liu, H., Carpenter, B.M., Marfurt, K.J., and Reches, Z., 2019, Analysis of fault damage zones using three-dimensional seismic coherence in the Anadarko Basin, Oklahoma: American Association of Petroleum Geologists Bulletin, v. 103, p. 1771–1785, https://doi.org/10.1306/1219181413417207.

Lobkovsky, A.E., Smith, B.A., Kudrolli, A., Mohrig, D.C., and Rothman, D.H., 2007, Erosive dynamics of channels incised by subsurface water flow: Journal of Geophysical Research, v. 112, F03S12, https://doi.org/10.1029/2006JF000517.

Micallef, A., Foglini, F., Le Bas, T., Angeletti, L., Maselli, V., Pasuto, A., and Taviani, M., 2013, The submerged paleolandscape of the Maltese Islands: Morphology, evolution and relation to Quaternary environmental change: Marine Geology, v. 335, p. 129–147, https://doi.org/10.1016/j.margeo.2012.10.017.

Micallef, A., et al., 2019, Active degassing across the Maltese Islands (Mediterranean Sea) and implications for its neotectonics: Marine and Petroleum Geology, v. 104, p. 361–374, https://doi.org/10.1016/j.marpetgeo.2019.03.033.

Micallef, A., et al., 2021, Groundwater erosion of coastal gullies along the Canterbury coast (New Zealand): A rapid and episodic process controlled by rainfall intensity and substrate variability: Earth Surface Dynamics, v. 9, p. 1–8, https://doi.org/10.5194/esurf-9-1-2021.

Nash, D.J., 1996, Groundwater sapping and valley development in the Hackness Hills, North Yorkshire, England: Earth Surface Processes and Landforms, v. 21, p. 781–795, https://doi.org/10.1002/(SICI)1096-9837(199609)21:9<781::AID-ESP616>3.0.CO;2-O.

Pedley, H.M., House, M.R., and Waugh, B., 1976, The geology of Malta and Gozo: Proceedings of the Geologists' Association, v. 87, p. 325–341, https://doi.org/10.1016/S0016-7878(76)80005-3.

Petroff, A.P., Devauchelle, O., Abrams, D.M., Lobkovsky, A.E., Kudrolli, A., and Rothman, D.H., 2011, Geometry of valley growth: Journal of Fluid Mechanics, v. 673, p. 245–254, https://doi.org/10.1017/S002211201100053X.

Roscoe, K.H., and Burland, J.B., 1968, On the generalised stress-strain behaviour of 'wet' clay, *in* Heyman, J., and Leckie, F.A., eds., Engineering Plasticity: Cambridge, UK, Cambridge University Press, p. 535–609.

Ryan, A.J., and Whipple, K.X., 2020, Amphitheatre-headed canyons of Southern Utah: Stratigraphic control of canyon morphology: Earth Surface Processes and Landforms, v. 45, p. 3607–3622, https://doi.org/10.1002/esp.4987.

Sagy, A., Reches, Z., and Roman, I., 2001, Dynamic fracturing: Field and experimental observations: Journal of Structural Geology, v. 23, p. 1223–1239, https://doi.org/10.1016/S0191-8141(00)00190-5.

Scheingross, J.S., and Lamb, M.P., 2017, A mechanistic model of waterfall plunge pool erosion into bedrock: Journal of Geophysical Research: Earth Surface, v. 122, p. 2079–2104, https://doi.org/10.1002/2017JF004195.

Printed in USA